International Journal of Mechanical Engineering Research and Technology

ISSN 2454-535X

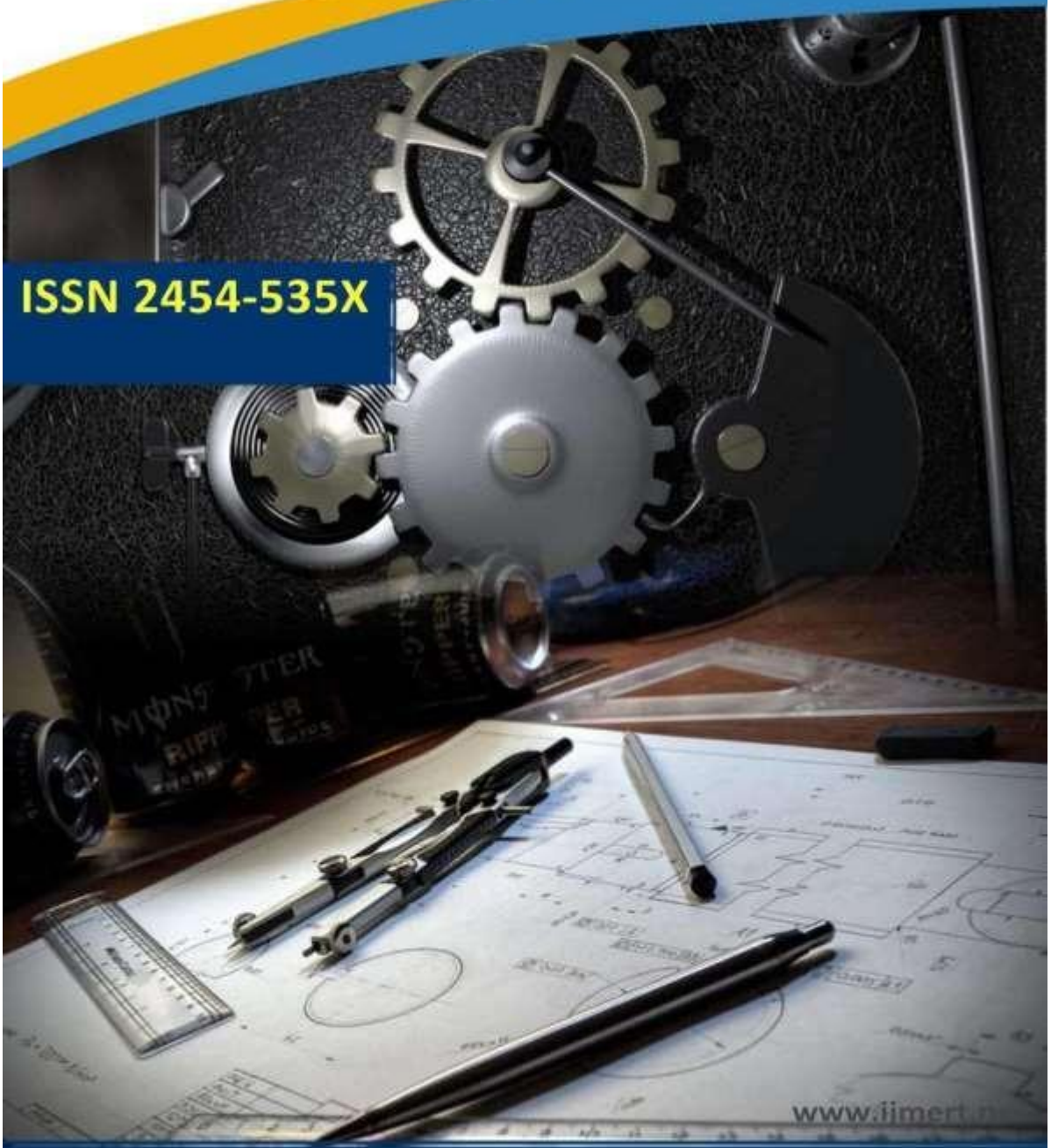

Email ID: info.ijmert@gmail.com or editor@ijmert.net

International Journal of Mechanical Engineering Research and Technology
ISSN 2454 – 5X
www.ijmert.co
Vol.13 Issue. 4, Oct 2021

Dynamic Analysis And Multi-Objective Optimization Of Slider-Crank Mechanism For An Innovative Fruit And Vegetable Washer

Nagamani. T., Danalaxmi, T. Mayuri, Priyanka

ABSTRACT For a very long time, the design of a wide variety of appliances and gadgets, including hand pumps, compressors, steam engines, internal combustion engines powered by gasoline and diesel, and many more, has made use of the slider-crank mechanism (SCM). Nonetheless, in order to reduce the inertial force effect on SCM, engineers still required to collaborate internationally. There are now two primary ways to achieve this. In the first case, counterweights are used; in the second, spring-damping systems are used, which result in spring-SCM. In reality, the inventive fruit and vegetable washer has effectively integrated the spring-SCM, which distinguishes it greatly from other models. This study carried out a dynamic analysis of spring-SCM under an external load.

KEYWORDS: Slider-crank mechanism, Spring, Dynamic analysis, Mechanism synthesis, Energy Consumption

INTRODUCTION

The concept of the slide-crank mechanism (SCM), which transforms rotation into linear movement, has been widely used in machine design and is currently used in a wide range of gadgets and appliances. Internal combustion engines running on gasoline and diesel, hand pumps, compressors, steam engines, feeders, crushers, punches, and injectors are a few examples of the applications [1-3]. Cycle forces and moment of inertia are two main problems with this mechanism, which lead to system vibrations and lower component fatigue strength. Reducing these forces is essential if the machine is to function well over an extended period of time and produce less noise.

Engineers from all around the world have been researching the dynamics of SCM to determine how to reduce shaking moment and shaking force [4-6]. A long time ago,

The concept of the slide-crank mechanism (SCM), which transforms rotation into linear movement, has been widely used in machine design and is currently used in a wide range of gadgets and appliances. Internal combustion engines running on gasoline and diesel, hand pumps, compressors, steam engines, feeders, crushers, punches, and injectors are a few examples of the applications [1-3]. Cycle forces and moment of inertia are two main problems with this mechanism, which lead to system vibrations and lower component fatigue strength. Reducing these forces is essential if the machine is to function well over an extended period of time and produce less noise.

Engineers from all around the world have been researching the dynamics of SCM to determine how to reduce shaking moment and shaking force [4-6]. A long time ago,

MATERIAL AND METHOD

SCM Model and Comprehensive Expressions

The model of SCM with spring, or spring-SCM, subjected to an external force F is illustrated in Figure 1. In this work, links are considered as rigid bodies, an ideal condition is applied to joint, at which friction is insignificant. The links OA and AB have length of l_1 and l_2, mass of m_1 and m_2, their gravity center being at C and G, respectively. A slider B owns a mass of m3, translates in the slot with an eccentricity Δ in relation to the rotational axis O of the drive motor. The constraint, i.e. $l_2 \geq l_1 + \Delta$, is applied so that the link OA in operation can rotate fully 360° without

International Journal of Mechanical Engineering Research and Technology
ISSN 2454 – 5X
www.ijmert.co
Vol.13 Issue. 4, Oct 2021

jamming. The average friction coefficient (both static and dynamic) between the slider and slot is designated as μ. In theory, the slider *B* undergoes an external force *F*, which includes several types *B* is an instant center *P* for velocities. In the generalized model, the gravity centers are located at certain position with the coordinates *u* and *v* in the local system x_1Oy_1 and x_2Ay_2 of the links OA and AB respectively. This allows for developing comprehensive expressions, which in practice could be useful for various links with different geometries (circular type of flywheel, rod type of crankshaft, ect.).

Assumed that *M* is torque of drive motor at joint *O* of link *OA*. The law of the torque determines rule and variation of kinetic parameters such as location, velocity, acceleration, and dynamics like D'alambert [22], and the expressions correlated kinematic and dynamic parameters are presented as

$$M \quad \frac{x_A y_B - x_B y_A}{x_A - x_B + s\mu\left(y_A - y_B\right)} F + \frac{1}{x_A - x_B + s\mu\left(y_A - y_B\right)} \left[\left(x_A + s\mu y_A\right)\left(I_{Gz\ AB} - m\, a_{Gx} y_G\right) - m_2\left(a_{Gy} + g\right)\left(x_A\left(x_B + s\ y_B\right) - x_G\left(x_A + s\mu y_A\right)\right) - m_3\left(x_A y_B - x_B y_A\right)\left(gs\mu + a_B\right) - m\, a_{Gx} y_A\left(x_B + s\mu y_B\right)\right] + I_{Cz} + m_1\left(x_C\left(a_{Cy} + g\right) - y_C a_{Cx}\right) \tag{1}$$

- Reactions at the joint *O*:

$$X_O \quad \frac{-\left(x_A \quad\right)}{x_A - x_B + s\mu\left(y_A - y_B\right)} F + m_1 a_{Cx} \frac{-1}{x_A - x_B + s\mu\left(y_A - y_B\right)} \left[s\mu I_{Gz\,AB} - \left(x_A - x_B\right)\left(m_3\left(g\mu s + a_B\right) + m\, a_{Gx}\right) - s\mu m_2\left(\left(a_{Gy} + g\right)\left(x_A - x_G\right) - a_{Gx}\left(y_B - y_G\right)\right)\right] \tag{2}$$

$$Y_O = \frac{-\left(y \quad y_B\right)}{x_A - x_B + s\mu\left(y_A - y_B\right)} F + m_1\left(a_{Cy} + g\right) + \frac{-1}{x_A - x_B + s\mu\left(y_A - y_B\right)} \left[I_{Gz\,AB}\varepsilon - m_2\left(a_{Gx}\left(y_A - y_G\right) - \left(a_{Gy} + g\right)\left(x_B - x_G\right)\right) - \left(y \quad - y \right)\left(m\ \mu s\left(a \quad + g\right) + m\left(\quad sg + a \right)\right)\right]_{2} \quad {}_{Gy} \quad {}_{A} \quad {}_{B} \tag{3}$$

of loading such as air resistance, springelasticitasell as other active loads.Sincetundergoes motion,the intersection of *OA* and the line perpendicular to the slot at reaction forces at joints of mechanism. Here, the most important task is to define the relation between dynamic (torque *M* and reactions) and kinematic (coordinate, velocity, angular and linear acceleration of links) parameters. Based on this, it allows for dealing with forward and inverse problems, or in other word the mechanism can be handled properly. For instance, if the motion law of the slider *B* is available, it is possible to define rotational angle φ law of the link *OA*, as well as law of *M*. Similarly, if there is law of the torque or rotational angle φ law, it is likely to determine the rest parameters. The main problem is solved by using dynamic principle

follows:

International Journal of Mechanical Engineering Research and Technology
ISSN 2454 – 5X
www.ijmert.co
Vol.13 Issue. 4, Oct 2021

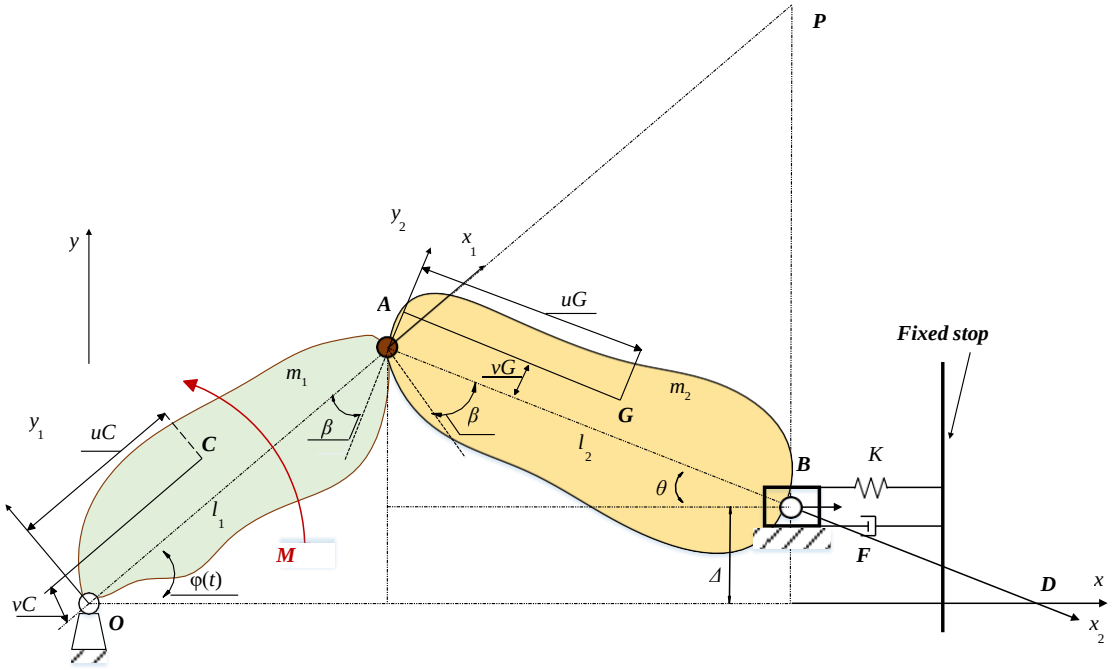

Figure 1. Modelization of slider-crank mechanism with spring.

- Reactions at the joint *A*:

$$X_A = \frac{(x_A - x_B)}{x_A - x_B + s\mu(y_A - y_B)}F + \frac{1}{x_A - x_B + s\mu(y_A - y_B)}\Big[s\mu I_{Gz\,AB}\varepsilon - (x_A - x_B)\big(m_3(g\mu s + a_B) + m_2 a_{Gx}\big) - s\mu m_2\big((a_{Gy} + g)(x_A - x_G) - a_{Gx}(y_B - y_G)\big)\Big] \quad (4)$$

$$Y_A = \frac{y_A - y_B}{x_A - x_B + s\mu(y_A - y_B)}F + \frac{1}{x_A - x_B + s\mu(y_A - y_B)}\Big[-I_{Gz\,AB}\varepsilon - m_2\big(a_{Gx}(y_A - y_G) - (a_{Gy} + g)(x_B - x_G)\big) - (y_A - y_B)\big(m_2\mu s(a_{Gy} + g) + m_3(\mu s g + a_B)\big)\Big] \quad (5)$$

- Reactions at the joint B:

International Journal of Mechanical Engineering Research and Technology
ISSN 2454 – 5X
www.ijmert.co
Vol.13 Issue. 4, Oct 2021

$$X_B = \frac{(x_A - x_B)}{x_A - x_B + s\mu(y_A - y_B)} F + \frac{1}{B} \left[s\mu I \varepsilon - x - x + s\mu(y - y) \right]_A^{Gz\ AB} - m_3(x_A - x_B)(g\mu s + a_B) - s\mu m_2\left((a_{Gy} + g)(x_A - x_G) - a_{Gx}(y_A - y_G)\right) | \quad (6)$$

$$\frac{y_A - y_B}{B} \frac{F}{x_A - x_B + s\mu(y_A - y_B)} + \frac{1}{x_A - x_B + s\mu(y_A - y_B)} \left[-I_{Gz\ AB} \varepsilon - m_2\left(a_{Gx}(y_A - y_G) - (a_{Gy} + g)(x_A - x_G)\right) \right] - m_3(y_A - y_B)(\mu s g + a_B) \quad (7)$$

• Reactions that the slot exerts on the slider *B* (perpendicular to the slot):

$$N_B = \frac{y_A - y_B}{x_A - x_B + s\mu(y_A - y_B)} F + \frac{1}{x_A - x_B + s\mu(y_A - y_B)} \left[-I_{Gz\ AB} \varepsilon - m_2\left(a_{Gx}(y_A - y_G) - (a_{Gy} + g)(x_A - x_G)\right) \right] - m_3\left((y_A - y_B)a_B - (x_A - x_B)g\right) \quad (8)$$

Details of components in the expressions (1-8) can be found in the Appendix below. Besides, I_{Cz} and I_{Gz} are mass moment of inertia of links *OA* and *AB* respectively about the axis *z* through gravity centers *C*, *G* of those two links; *g* – gravitational acceleration.

Looking into the abovementioned expressions, it is observed that there are two separate parts. One depends upon the load *F*, which is alterable while the structure in operation, it seems to be a factor causing system variation. The other contains available parameters of the structure such as mass, moment of inertia, friction coefficient. It is evident that the other parameters including coordinates of points (*A*, *B*, *C*, *G*), linear and angular acceleration of links (*OA*, *AB*, *B*) can be changed during operation, but they also depend on angular coordinate and acceleration of link *OA* (φ, φ''), thus they seem to be available. In order to manipulate the aforementioned structure, the expressions should be turned into systems of differential equations, so that they can be solved by numerical method appropriately.

From the expressions (2-7), it results in:

$$X_O = -X_A + m_1 a_{Cx};\ Y_O = -Y_A + m_1(a_{Cy} + g)\ \ X_B = X_A + m_2 a_{Gx};\ Y_B = Y_A + m_2(a_{Gy} + g) \quad (9)$$

The magnitude of these reaction forces (in the expression (9)) presents a small discrepancy, which depends on mass m_1, m_2 and acceleration of gravity centers *C*, *G*. Indeed, the aforementioned expressions (1-8) can be used for solving not only forward problems (motion rule deduces law of the torque), but also inverse problems (based on law of the torque, it is possible to find motion rule). Dynamic expressions are built to apply straightforwardly to control the structure. Yet, the outcomes in analytical form allow for dealing with optimization design of the system at any criteria. Next section presents the application of spring-SCM for an innovative fruit and vegetable washer. By using theoretical basis mentioned in this

International Journal of Mechanical Engineering Research and Technology
ISSN 2454 – 5X
www.ijmert.co
Vol.13 Issue. 4, Oct 2021

section, dynamic feature of the washer could be analyzed in order to optimize several parameters of the system.

Application of Spring-SCM for Designing an Innovative Fruit and Vegetable Washer

Illustration of the washer with spring-SCM is shown in Figure 2 [23]. This washer works on the basis of two main motions of drum (container of fruit and vegetable) including horizontal shaking and rotational. The former is the most important one, which helps to remove most of dirt from fruit and vegetable. This horizontal shaking motion is created by spring-SCM, which is a key know-how that makes this washer different from the existing ones [24 – 26]. Scheme of horizontal shaking motion of the washer is demonstrated in Figure 3. Spring system is modeled by using a single spring with an equivalent stiffness *K*.The SCM (2) converts the rotation of a drive motor to linear motion of the slider, which then generates anactive impact of the drum on the vegetables/fruits. The drum (3) performs horizontal shaking (frequency *f* = 1 - 2 Hz, Amplitude *A* = 0.05 - 0.1 m), repeatedly actuated by the drive motor (angular velocity ω_2 rad/s). The spring system is continuously compressed and stretched to conserve and release potential energy. The parameters of SCM used for the washer are included in Table 1.

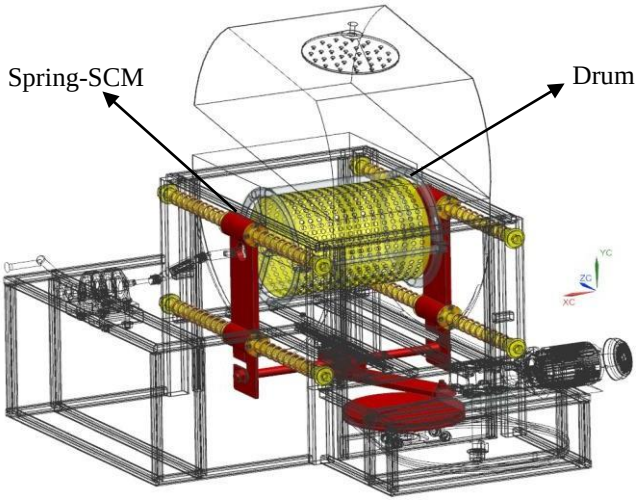

Figure 2. Modeling of multifunctional washer with spring-SCM [23]

In particular, rotational angle law of link *OA* owns an uniform transformation: $\varphi = \varphi_0 + \omega_0 t + \varepsilon_0 t^2/2$. Since there is an eccentricity $\Delta=0$, hence there is $A=l_1$. In the model, apart from spring elasticity, the most significant external force is yielded from water resistance while the drum being in horizontal shaking motion. To analyze this, the fluid dynamics theory is applied. Assumed that the drum is an approximate cylinder with cross-section radius *R* and length *L*, and it is half flooded in the water. The drag force F_c exerting on the drum can be derived by following formula [26]:

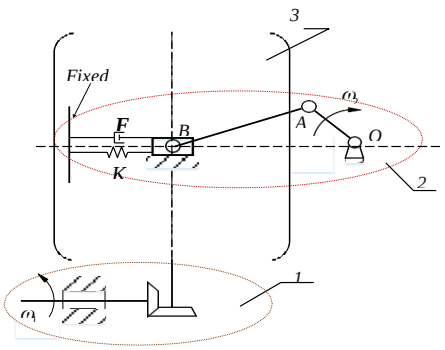

International Journal of Mechanical Engineering Research and Technology
ISSN 2454 – 5X
www.ijmert.co
Vol.13 Issue. 4, Oct 2021

Figure 3. Principle scheme of the washer: 1) System to create rotational motion of drum; 2) Spring-SCM; 3) Drum.

Table 1. Parameters of SCM used for an innovative fruit and vegetable washer

Parameter	**Units**	**Magnitude**
l_1	m	0.1
l_2	m	0.2
m_1	kg	0.035
m_2	kg	0.066
m_3	kg	12
μ	-	0
g	m/s^2	9.81
Δ	m	0
I_{Cz}	kg.m^2	40.168 •10^{-6}
I_{Gz}	kg.m^2	255.548•10^{-6}
φ_0	rad	0
f	Hz	2
ε_0	rad/s^2	0
ω_0	rad/s	4π
A	m	0.1
k	N/m	1000

$$F_x = \frac{1}{2} \cdot C_B \cdot S \cdot \rho \cdot v^2 \quad (10)$$

International Journal of Mechanical Engineering Research and Technology
ISSN 2454 – 5X
www.ijmert.co
Vol.13 Issue. 4, Oct 2021

Where: C_x – the drag force coefficient, which is obtained from experiments; S – longitudinal cross-section area; ρ – density of water; v_B – velocity of drum.

The relation between C_x and factor Reynolds (Re) corresponding to a circular cylinder in a flow normal to the axis is described in details in Ref. [27], where Reynolds is defined as follows:

In particular, the diameter of drum D= 0.4 m, and dynamic viscosity coefficient of water $\eta = 8.9 \cdot 10^{-4}\ \mathrm{kg/m \cdot s}$. With the input parameters: S=0.32 m^2, $\rho = 1000\ kg/m^3$, it is possible to derive the factor Reynolds $Re = 3.6 \cdot 10^5$. C_x equals approximately to 1.2 according to Ref. [28]. Based on the expression (10), the drag force $F_c \approx 50\ \mathrm{N}$. From this, the resistance force F in the expressions (1-8) for the model of the washer is:

$$F = -K\left(x_B - l_2\right) - sF_c - s\mu N_B \tag{12}$$

Where, $s = signum\left(v_B\right) = \pm$, this function defines sign and direction of slider B motion. In the washer model, since the drum slides horizontally on the linear bearing, fiction is minor or ($\mu \approx 0$). From the expression (12), it results in: $F = -K\left(x_B - l_2\right) - sF_c$. By substituting the expression (12) into the expressions (1-8), it is possible to analyze eight dynamic parameters of the washer.

Moreover, in case there is a friction at the slider B, firstly it needs to substitute the expression (12) into (8) in order to determine the final expression of N_B. This expression is then substituted back again into (12). Eventually, based on the new defined expression (12), it is possible to determine necessary parameters in accordance with the expressions (1-7).

RESULTS AND DISCUSSION

Here, the kinematic and dynamic characteristic of spring-SCM is analyzed on the basis of comprehensive expressions (1-8) and input parameters included in Table 1. For the case when spring stiffness K=1000 N/m, angular velocity $\omega = 4\pi = const$, initial condition $\varphi(0)$=0, it turns our that the three points O, A, B are one an identical line (*A is in the middle of O* and B) and the spring is compressed with a distance equal to the length of link OA.

Dynamic Characteristic of the Fruit and Vegetable Washer

When T=1s, dynamic characteristic of reactions at joints O, A and B can be observed in Figure 4, Figure 5 and Figure 6 respectively. It is noteworthy that at the initial time t_0=0, angle φ_0=0, three points O, A, B are on an identical line, where the point B is the further from the point O. In this case, spring is compressed the most by axis x (axially), thus there is no reaction force by axis y (Y=0) at the joints, while reaction force reaches to the maximum value by axis x: X_{Amax} = 235.56 N, X_{Bmax} = 234.24 N, X_{Omax} = 235.83 N. Reaction forces in both of x and y direction at the joints has a similar characteristic, but there is a small difference in magnitude and direction among joints O, A and B. At the time period t = 0.364 s, reaction by axis y of all three reaches the maximum value: Y_{Amax} = 80.84 N, Y_{Bmax} = 79.67 N, Y_{Omax} = 81.46 N. If the reaction force magnitude is reduced, life service of bearings and system parts will be longer. The graph of the overall reaction forces $R_{O/A/B} = \sqrt{X^2_{O/A/B} + Y^2_{O/A/B}}$ is illustrated in Figure 7.

International Journal of Mechanical Engineering Research and Technology
ISSN 2454 – 5X
www.ijmert.co
Vol.13 Issue. 4, Oct 2021

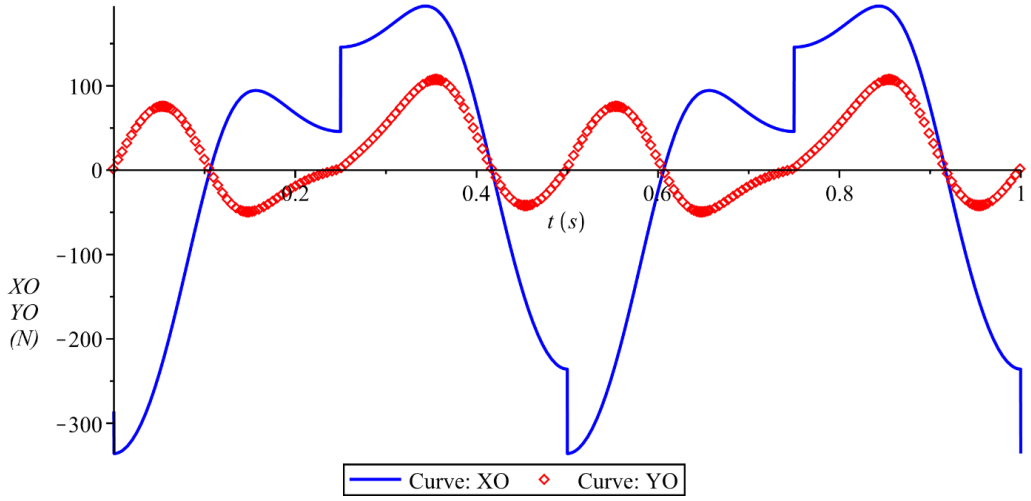

Figure 4. Reaction forces at joint *O*

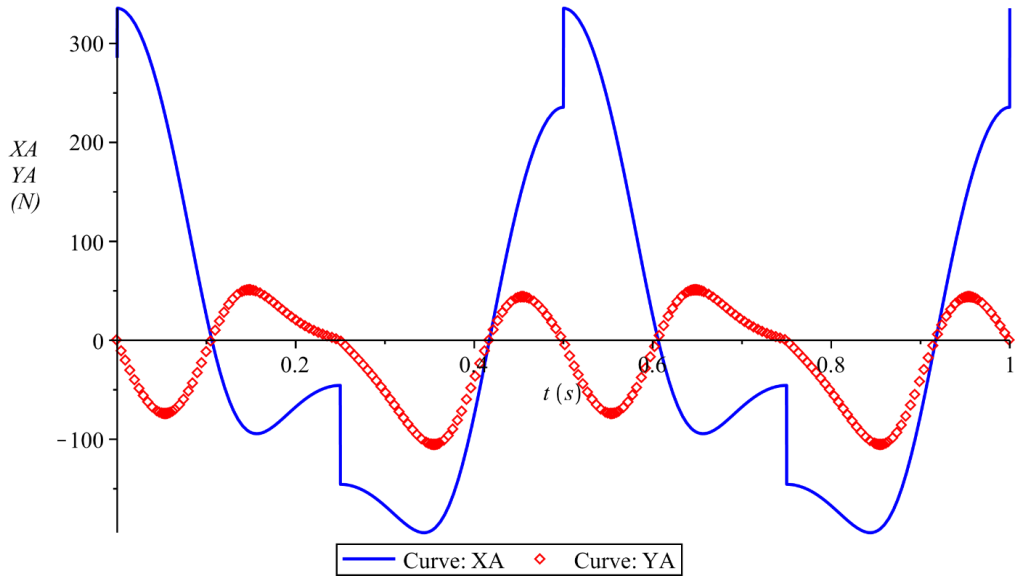

Figure 5. Reaction forces at joint *A*

International Journal of Mechanical Engineering Research and Technology
ISSN 2454 – 5X
www.ijmert.co
Vol.13 Issue. 4, Oct 2021

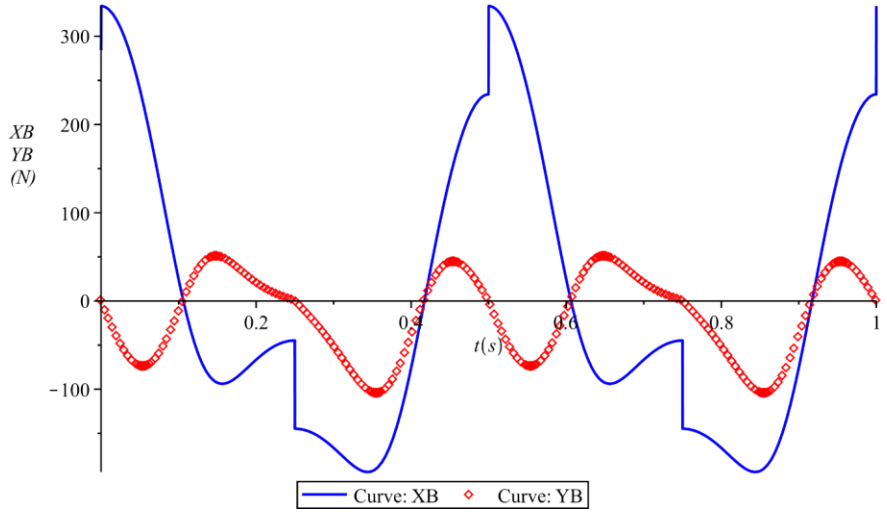

Figure 6. Reaction forces at joint *B*

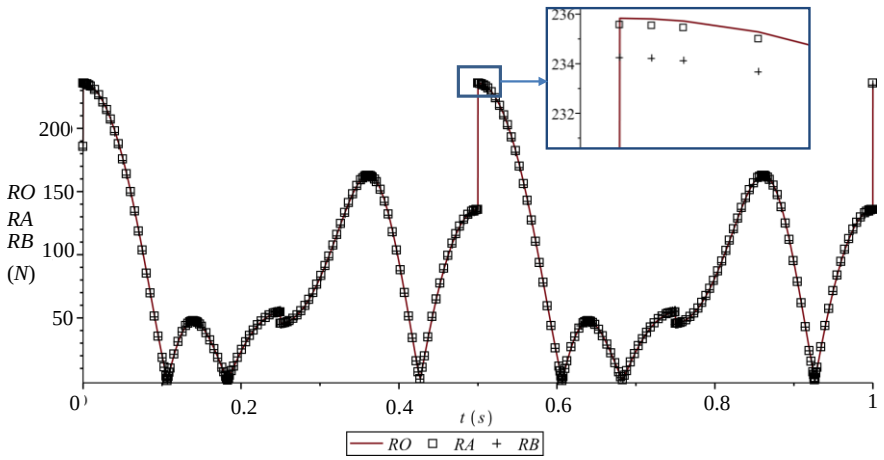

Figure 7. Overall reaction forces at joints *O*, *A*, *B*

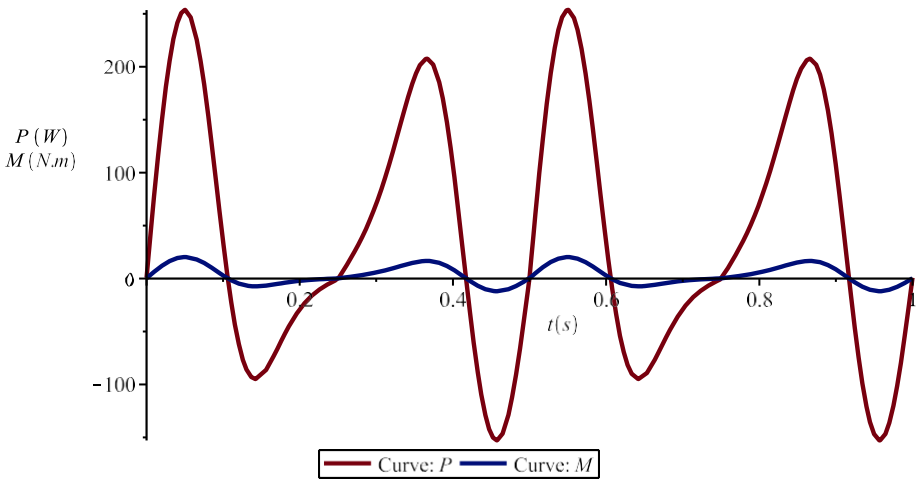

International Journal of Mechanical Engineering Research and Technology
ISSN 2454 – 5X
www.ijmert.co
Vol.13 Issue. 4, Oct 2021

Figure 8. Characteristic of torque *M* and power *P* of rotary motor

The graphs in Figure 4 - Figure 7 play a crucial role in designing joints *O*, *A* and *B*, they also present a regular tendency and an abrupt increment. This causes shear stress of joint shaft to alter and accumulate, resulting in fatigue and failure afterward. However, Figure 7 shows that among those three joints there is no huge differences in reaction magnitude and tendency. Regarding the elaboration, the joint *A* seems to be the smallest one, connecting several parts (links *OA*, *AB*, bolts, ect.), that would be the most vulnerable one. Thus, the reaction R_A should be analyzed in more details. Characteristic of torque *M* and power *P* of the drive motor is demonstrated in Figure 8. It shows that as spring stiffness *K*=1000 N/m, maximum value of power or P_{max} = 253.51 *W* is achieved at time period *t* = 0.05 s. P_{max} is frequently used for selecting a suitable drive motor. Yet, P_{max} is also a required power to secure that the system works properly, hence it presents an indicator of overall energy consumption, which needs to be minimized.

Effect of Spring Stiffness K on Torque and Reaction Forces

For this specific study on the innovative fruit and vegetable washer, spring stiffness *K* is set in the range of 0 ... 3650 N/m. Correlation among P_{max}, reaction forces at joint A $\left(R_A = \sqrt{X_A^2 + Y_A^2}\right)$ and stiffness *K* is presented in Figure 9. It shows that the power *P* reduces significantly from 253.52 W (when *K*=0) to 132.99 W (when *K*=2623.85 N/m). This points out that the use of spring has a positive effect on diminishing the required power of drive motor, which implies less energy consumption and more economical motor. The optimal value of spring stiffness to minimize power is 2623.85 N/m.

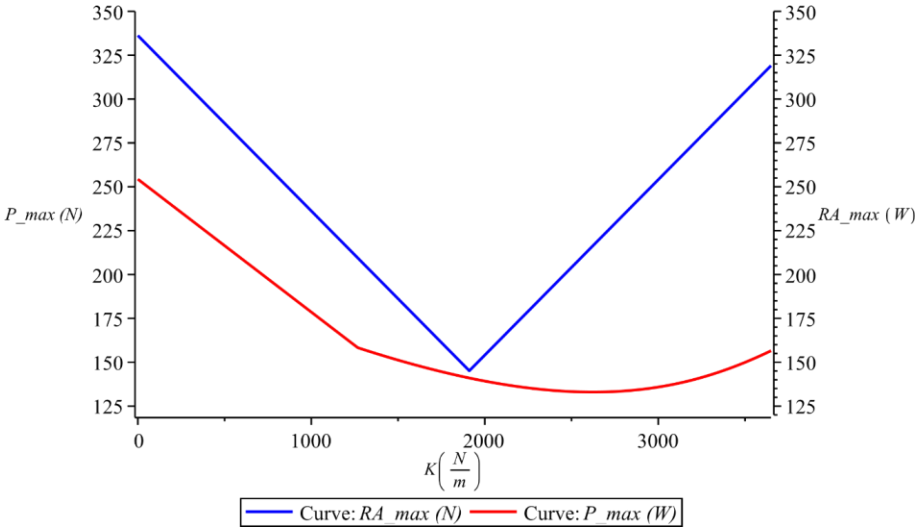

Figure 9. Effect of spring stiffness *K* on the required power of drive motor P_{max}

Since the reaction forces at joints *O, A, B* has similar characteristic, their dependence upon spring stiffness *K* seems to be identical. With the considered range of *K*, spring's role in reduction of reaction forces is revealed evidently. When spring is not used or *K*=0, reaction forces are always higher than that of the case using spring or 0 < K < 3650. To minimize reaction, the optimal value of spring stiffness is in the range of 1895-1920 N/m. The calculation results obtained by numerical method are provided in Table 2.

Table 2. Summary of results obtained from numerical method

International Journal of Mechanical Engineering Research and Technology
ISSN 2454 – 5X
www.ijmert.co
Vol.13 Issue. 4, Oct 2021

	Reaction forces		**Power**	
	R_O (N)	R_A (N)	R_B (N)	P (W)
Mechanism without K	337.012	336.22	334.24	253.52
Mechanism with K	145.15 (K_{OPT} = 1918.65 N/M)	145.14 (K_{OPT} = 1910.76 N/M)	144.75 (K_{OPT} = 1894.96 N/M)	132.99 (K_{OPT} = 2623.85 N/M)
% reduction	**56.93 %**	**56.83 %**	**56.69 %**	**47.54 %**

Multi-objective Optimization of Spring-SCM

Although there are many studies on SCM features, a few of them are regarded to optimization of motor power and reaction forces [29, 30]. Khemilia et al. [29] carried out the multi-objective optimization of SCM by using two approaches such as genetic algorithm and particle swarm optimization. While, Chandrakar et al. [30] optimized the performance of kinematic and dynamic effect of SCM with the aim to reduce energy consumption, joint reaction and processing material cost. Based on the literature review, the authors intend to optimize both of motor power P and reaction forces at joint A (R_A) by using weight method. Assumed that Φ is an equivalent function as follows:

$$\Phi(w,K) = w\cdot\frac{P_{\max}(K)}{\max\left[P_{\max}(K)\right]} + (1-w)\cdot\frac{R_{A\max}(K)}{\max\left[R_{A\max}(K)\right]} \to \min \tag{13}$$

Where, w is weight coefficients, varying in the range of 0 ÷ 1. It needs to analyze a function of two variables $\Phi(w, K)$ to determine a Pareto curve. With every value of w, it is possible to define Φ_{min} and spring stiffness K. Eventually, the outcome of optimal values can be achieved. Figure 10 depicts Pareto curve (in red), which is the optimizing result of P and R_A in spring-SCM.

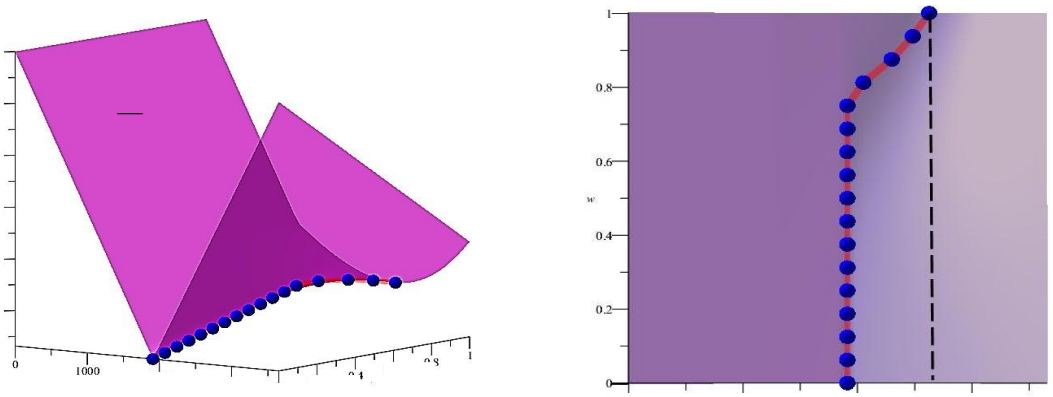

International Journal of Mechanical Engineering Research and Technology
ISSN 2454 – 5X
www.ijmert.co
Vol.13 Issue. 4, Oct 2021

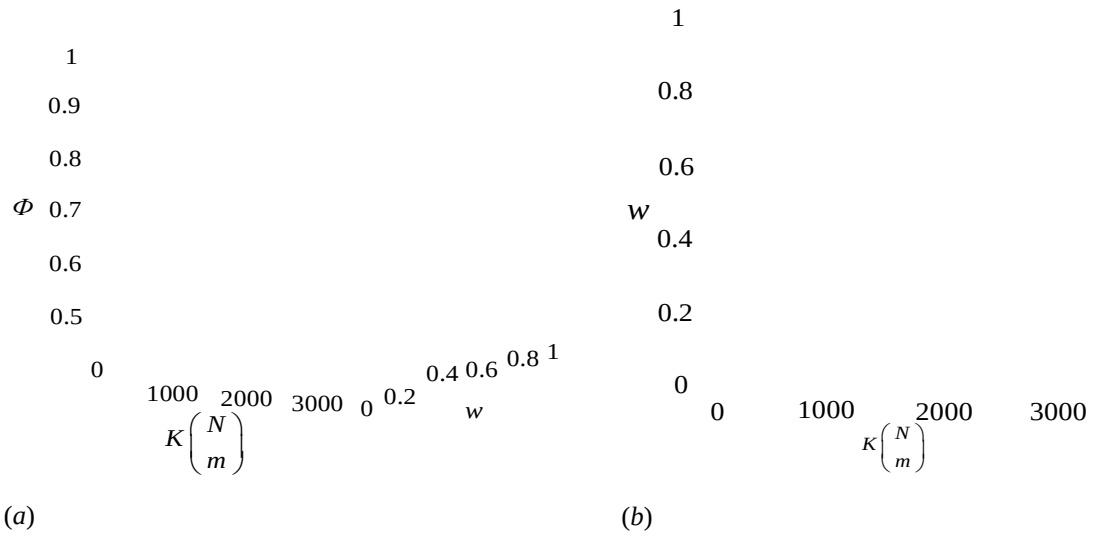

Figure 10. Illustration of Pareto optimality in two-objective (*P* and *R*) optimization: a) 3D view; b) Plane *w*-*K*

Depending on the priority order of *P* and *R* in the design process of SCM, an engineer would select a suitable value of *w*. For every input data of *w*, it is possible to define spring stiffness *K*, P_{max} or optimal motor power, as well as optimal reaction forces R_A. Looking into Table 3 and Figure 10b, it is observed that as *w* varies in the range of 0-0.75, it would not influence on the extreme of *P* and R_A. This indicates that *K* varying in the range of 1910-2624 N/m plays an important role in both energy saving and long-term life service of SCM. However, if *K*=1990.4 N/m, at *w*=0.8, the optimizing percentage of *P* is 45% (close to the maximum value of 47.54 %) and that of R_A is 54.5% (close to the maximum value of 56.83%). Although in theory these values (*P* and R_A) vary depending on SCM parameters such as mass, link length, moment of inertia, ect., the selection of spring stiffness *K* based on multi-objective optimization could be the most appropriate way, when weight value *w* varies.

Table 3. Multi-objective optimization results in accordance with *w*

w	*K* (*N/m*)	*P_max* (*W*)	*Optimizing percentage of P*	R_A*_max* (*N*)	*Optimizing percentage of* R_A
0	1910.76	141.02	44.38%	145.14	56.83%
0.25	1910.76	141.02	44.38%	145.14	56.83%
0.5	1910.76	141.02	44.38%	145.14	56.83%
0.75	1910.76	141.02	44.38%	145.14	56.83%
0.8	1990.4	139.44	45%	153.11	54.46%
0.9	2377.38	134.06	47.12%	191.81	42.95%
1	2623.86	132.99	47.54%	216.45	35.62%

International Journal of Mechanical Engineering Research and Technology
ISSN 2454 – 5X
www.ijmert.co
Vol.13 Issue. 4, Oct 2021

Verification by NX Motion Simulation RecurDyn® Software

In order to verify the results, a spring-SCM is modeled and simulated by means of NX Motion Simulation-RecurDyn® software, as shown in Figure 11. Figure 12 and Figure 13, which demonstrate law of reaction forces at joint *A* and torque obtained from two methods: one is analytical (based on expressions (1), (4) and (5)), the other is numerical (NX Software). Taking into account, spring stiffness K=1990.4 N/m and drag force is of 50 N.

It is observed that both methods (analytical and numerical) yield identical results. The maximum value of R_A from NX Software is 153.51 N at time period t=0.75 s (deviation in comparison with that of analytical method is 0.26%). While, maximum value of torque from NX Software is 11.0797 N.m at time period t=0.885 s, corresponding to P_{max}=139.23 *W* (deviation in comparison with that of analytical method is 0.15%). This proves the correctness and reliability of comprehensive expressions (1÷8), which were developed in this work, as well as the results included into Table 2 and Table 3 are feasible. Besides, thanks to multiobjective optimization design for spring-SCM with K=1990.4 N/m, the innovative fruit and vegetable washer could be elaborated by using an optimal drive motor, which consumes 45% less nergy, and a reduction of 55% in reaction forces at joints of the mechanism can be achieved.

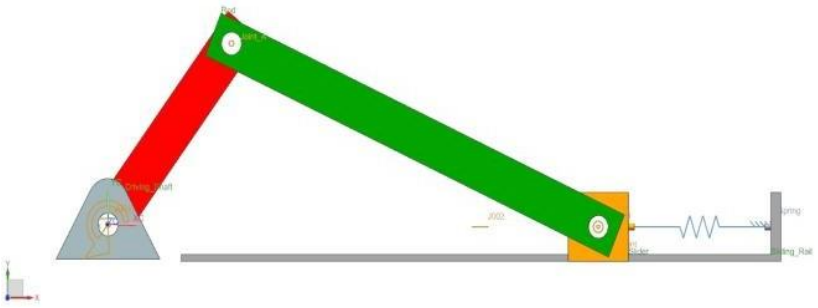

Figure 11. Spring-SCM model in NX Motion Simulation

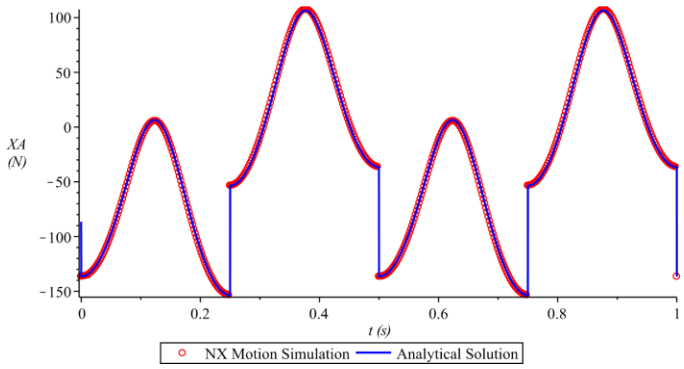

International Journal of Mechanical Engineering Research and Technology
ISSN 2454 – 5X
www.ijmert.co
Vol.13 Issue. 4, Oct 2021

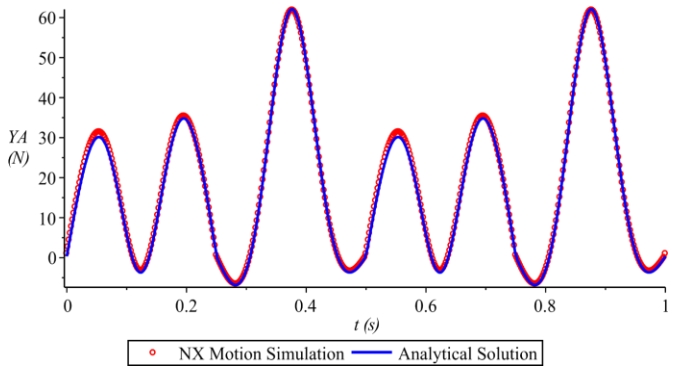

Figure 12. Characteristic of reaction forces at joint *A*

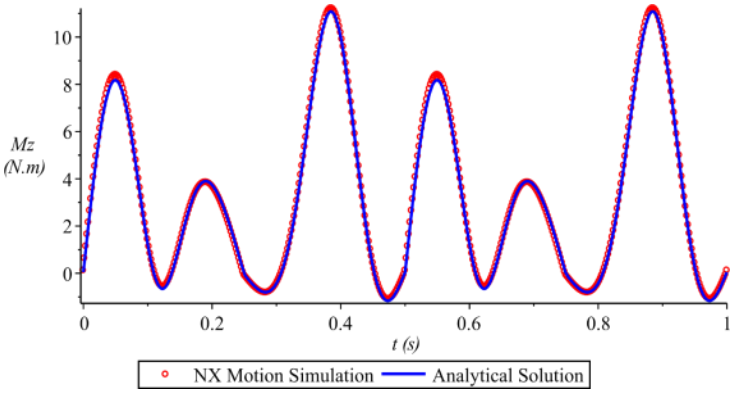

Figure 13. Characteristic of input required torque

International Journal of Mechanical Engineering Research and Technology
ISSN 2454 – 5X
www.ijmert.co
Vol.13 Issue. 4, Oct 2021

CONCLUSIONS

Comprehensive study on dynamic characteristic of spring-SCM showed that the spring stiffness section is an important step, resulting in a significant reduction of reaction forces at joints and power of the drive motor attached to the crank. This know-how was applied to an innovative fruit and vegetable washer with the principal difference being horizontal shaking motion of drum. The optimization problem of two criteria, i.e. reaction forces at joints and consuming power of drive motor, was solved. Thank to this, the optimal spring stiffness was obtained. Moreover, the analytical results were in agreement with numerical one from NX Motion Simulation-RecurDyn® software. The outcomes from this work can also be implemented straightforwardly for designing not only the washer, but also other useful mechanical devices, in which SCM is used.

Appendix

$$\begin{cases} \varphi_{OA} = \varphi = \varphi(t); \\ \omega_{OA} = \omega = \dfrac{d}{dt}\varphi(t) = \varphi'(t); \\ \varepsilon_{OA} = \varepsilon = \dfrac{d^2}{dt^2}\varphi(t) = \varphi''(t) \end{cases}$$

Angular coordinate, velocity, acceleration of the link *OA*

$$x_A = l_1\cos\varphi;\ y_A = l_1\sin\varphi$$

Joint *A* coordinates

$$x_B = x_A + \sqrt{l_2^2 - (y_A - \Delta)^2};\quad y_B = \Delta = const$$

Slider *B* coordinates

$$x_C = \cos\varphi\cdot u_C - \sin\varphi\cdot v_C;\quad y_C = \sin\varphi\cdot u_C + \cos\varphi\cdot v_C$$

Gravity center *C* coordinates of link *OA*

$$\sin\theta = \frac{y_A - \Delta}{l_2};\ \cos\theta = \sqrt{1-(\sin\theta)^2}$$

Sine and cosine of the angle θ, formed by link *AB* and horizontal direction as shown in Figure 1.

$$\begin{cases} x_G = x_A + \cos\theta\cdot u_G + \sin\theta\cdot v_G \\ y_G = y_A - \sin\theta\cdot u_G + \cos\theta\cdot v_G \end{cases}$$

Gravity center *G* coordinat

$$v_{B\,Cx\,Cy\,Gx\,Gy} = \frac{d}{dt}(x_B\ x_C\ y_C\ x_G\ y_G) = f_{1\div5}(\varphi,\varphi')$$

$$a_{B\,Cx\,Cy\,Gx\,Gy} = \frac{d^2}{dt^2}(x_B\ x_C\ y_C\ x_G\ y_G) = f_{6\div10}(\varphi,\varphi',\varphi'')$$

Velocity and acceleration respectively.

$$\omega_{AB} = \frac{v_B}{PB} = \frac{v_B}{x_B\tan\varphi - \Delta} = f_{11}(\varphi,\varphi')$$

$$\varepsilon_{AB} = \frac{d}{dt}\omega_{AB} = f_{12}(\varphi,\varphi',\varphi'')$$

Angular velocity and accel

$$s = signum(v_B) = \pm$$

This function determines s any time *t*. As the slider m and vice versa.

Nomenclature

F	external force	N
S	cross-section area of drum	cm^2

Greek letters

η	viscosity coefficient of water	kg/m×s
μ	frictiondensity of water	kg/m^3
ρ		
ω	angular velocity	rad/s

Subscription

opt	optimized
max	maximum

ACKNOWLEDGMENT

The authors would like to express their gratitude to Rector of Industrial University of Ho Chi Minh City and colleagues at Faculty of Mechanical Engineering for the interest, help and invaluable contributions tothe paper.

REFERENCES

[1] M. Calisti, F. Corucci, A. Arienti, and C. Laschi, "Dynamics of underwater legged locomotion: modeling and experimentson an octopus-inspired robot," *Bioinspir. Biomim.*, vol 10, no. 4, pp. 1- 15, 2015.

International Journal of Mechanical Engineering Research and Technology
ISSN 2454 – 5X
www.ijmert.co
Vol.13 Issue. 4, Oct 2021

[2] Z. Deng, Y. Liu, L. Ding, H. Gao, H. Yu, and Z. Liu, "Motion planning and simulation verification of a hydraulic hexapod robot based on reducing energy/flow consumption," *J Mech Sci Technol*, vol. 29, no. 10, pp. 4427–4436, 2015.

[3] K. Koser, "A slider crank mechanism based robot arm performance and dynamic analysis," *Mech Mach Theory*, vol. 39, no. 2, pp. 169–182, 2004.

[4] S. Akbari, F. Fallahi, and T. Pirbodaghi, "Dynamic Analysis and Controller Design for a Slider– crank Mechanism with Piezoelectric Actuators," *J Comput Des Eng*, vol. 3, no. 4, pp. 312-321, 2016.

[5] Y. Li, G. Chen, D. Sun, Y. Gao, and K. Wang, "Dynamic analysis and optimization design of a planar slider–crank mechanism with flexible components and two clearance joints," *Mech Mach Theory*, vol. 99, pp. 37-57, 2016.

[6] V. H. Arakelian and M. R. Smith, "Shaking force and shaking moment balancing of mechanisms: A historical review with new examples," *J Mech Des*, vol. 127, pp. 334–339, 2005.

[7] F. L. Conte, G. R. George, R. W. Mayne and J. P. Sadler, "Optimum mechanism design combining kinematic and dynamic-force considerations," *ASME Transactions, J Eng for Industry, Series B*, Vol. 95, no. 2, pp. 662–670, 1975.

[8] K. A. Ansari and N. U. Khan, "Nonlinear vibrations of a slider-crank mechanism," *Appl Math Model*, vol. 10, no. 2, pp. 114–118, 1986.

[9] J.L. Ha, R. F. Fung, K. Y. Chen, and S. C. Hsien, "Dynamic modeling and identification of a slider-crank mechanism," *J Sound Vib.*, vol. 289, no. 4-5, pp. 1019–1044, 2006

[10] V. H. Arakelian and S. Briot, *Balancing of linkages and robot manipulators: Advanced Methods with Illustrative Examples*, Berlin, Germany: Springer-Verlag, 2015.

[11] Y. L. Gheronimus, "An approximate method of calculating a counterweight for the balancing of vertical inertia forces," *J Mech*, vol. 3, no. 4, pp. 283-288, 1968.

[12] D. N. Cambell, "Balanced crank mechanism," GB Patent 1 551 600, August 30, 1979.

[13] B. D. Frischknecht, L. L. Howell, and S. P. Magleby, "Crank-slider with spring constant force mechanism," *Proceedings of the ASME Design Engineering Technical Conferences*, p. 120-135. 2004

[14] D. Tarnita and D. Bolcu, "Contributions on the dynamic synthesis of crank-slider mechanisms actuated by springs," *12th IFToMM World Congress*, p. 35-45, 2007

[15] B. D. Jensen and L. L. Howell, "Bistable Configurations of Compliant Mechanisms Modeled Using Four Links and Translational Joints," *ASME. J. Mech. Des.*, vol. 126, no. 4, pp.657-666, 2004.

[16] Q. Tian, P. Flores, and H. M. Lankarani, "A comprehensive survey of the analytical, numerical and experimental methodologies for dynamics of multibody mechanical systems with clearance or imperfect joints," *Mech Mach Theory*, vol. 122, pp. 1–57, 2018.

[17] K. D. Joseph, "Analysis and Synthesis of slider crank mechanism with a flexibly attached slider,"

International Journal of Mechanical Engineering Research and Technology
ISSN 2454 – 5X
www.ijmert.co
Vol.13 Issue. 4, Oct 2021

J Mech, vol. 5, pp. 239-247, 1970.

[18] D. Groza, "Balancing of a Slider-Crank Mechanism by Using a Counter Mass and a Progressive Spring with Two Rates," *Appl Mech Mat*, vol. 823, pp. 37-42, 2016

[19] D. Chang, J. Kim, D. Choi, K. J. Cho, T. Seo, and J. Kim, "Design of a slider-crank leg mechanism for mobile hopping robotic platforms," *J. Mech. Sci. Technol.*, vol. 27, no. 1, pp. 207– 214, 2013.

[20] L. Mariti, V. H. Mucino, E. Pennestri, A. Cavezza, M. Gautam, P. P. Valentini, "Optimization of a high-speed deployment slider–crank mechanism: A design charts approach," *J Mech Des*, vol. 136, no. 7, pp. 1-7, 2014.

[21] A. A. Jomartov, S. U. Joldasbekov, and Y. M. Drakunov, "Dynamic synthesis of machine with slider-crank mechanism," *Mech. Sci.*, vol. 6, no. 1, pp. 35-40, 2015.

[22] R.C. Hibbeler. Engineering Mechanics: Dynamics. 14th ed. Pearson Education Inc., 2016.

[23] H. M. Dang, V. B. Phung, V. D. Nguyen, and T. T. Tran, "Multifunctional fruit and vegetable washer," *VN Patent Application* № VN2019324A2, 2019 (In submission)

[31] 1709 – 1712, 2015.

[24] C.H. Wang and S. Taishan, "Water-saving type fruit and vegetable washing and disinfecting method and device," EU Patent Application, № EP2005846A1, 2007.

[25] D. K. Lewis, "Method and Apparatus for Washing Fruits and Vegetables," *US Patent № US* 20090151749A1, 2009.

[26] M. E. Hoye, "Portable Fruit and Vegetable Washer," US Patent №. US2017/0135527A1, 2017.

[27] G. Shlikhting, "Boundary layer theory – Translate from German," Main edition of the physical and mathematical literature of publishing "Science", Moscow, 1974.

[28] S.F. Hoerner, "Fluid Dynamic Drag: Theoretical, Experimental and Statistical Information," *Hoerner Fluid Dynamics*, 1965

[29] I. Khemili, M. A. B. Abdallah, and N. Aifaoui, "Multi-objective optimization of a flexible slider-crank mechanism synthesis, based on dynamic responses," *Eng Optimiz*, vol. 51, no. 6, pp. 978-999, 2019.

[30] B. Chandrakar and M. M. Soni, "Design and Optimization of Slider and Crank Mechanism with Multibody Systems," *Int J Sci Res*, vol. 4, no. 6, pp.